ORIGINAL RESEARCH

The inhibitory effect of oridonin on colon cancer was mediated by deactivation of TGF-β1/Smads-PAI-1 signaling pathway in vitro and vivo

He-Qi Bu
Feng Shen
Junhui Cui

Department of Coloproctological Surgery, Tongde Hospital of Zhejiang Province, Hangzhou 310012, People's Republic of China

Background: Oridonin, the main active component of Rabdosia rubescens, has been demonstrated to have anti-tumor effect on all kinds of cancer cells through various mechanisms and it has shown antitumor activity in some tumors partially via the suppression of TGF-β/Smads signaling pathway. The aim of this study was to explore the anticancer effect of oridonin on human colon carcinoma and underlying mechanism in vitro and vivo.
Methods: CCK-8 assay was employed to assess cell viability. The key target genes and proteins involved in TGF-β/Smads pathway was detected by RT-PCR, Western blotting and immunohistochemistry. The orthotopic transplantation tumor model of colon cance LOVO cell was introduced to detect anti-cancer effects in vivo.
Results: Oridonin inhibited the proliferation of colon cancer LOVO cells in a concentration and time dependent manner. In addition, oridonin reduced the levels of Smad2, Smad3, Smad4, PAI-1 and the phosphorylation of Smad2 and Smad3 induced by TGF-β1 in vitro. Subsequently, we established an orthotopically implanted tumor model in nude mice and found that oridonin treatment significantly suppressed tumor growth, and which was accompanied by the down-regulation of Smad2, Smad3, Smad4, PAI-1 and p-Smad2, p-Smad3 expression levels.
Conclusion: Our present study demonstrated that the growth inhibition of colon cancer by oridonin could be partially mediated through discontinuing TGF-β1/Smads-PAI-1 signaling pathway, suggesting it as a promising agent in treating colorectal cancer.
**Keywords:** oridonin, colon cancer, TGF-β/Smads pathway, PAI-1

Introduction

Colorectal cancer (CRC) is the most common malignant tumor of the digestive tract, and the primary cause of cancer related deaths worldwide.[1] In China, CRC is the fifth and third most commonly diagnosed cancer in males and females respectively, and is the fifth leading cause of cancer-related deaths in both sexes.[2] It is a multifactorial disease,[3] and routinely managed by chemotherapy, radiotherapy, immunotherapy and surgery. Despite recent progress in therapeutic modalities however, the 5-year overall survival rate for advanced stage CRC remains low due to tumor recurrence and metastasis.[4] In addition, chemotherapy and radiotherapy are associated with severe toxicity, which significantly affects the patients' quality of life. Therefore, it is essential to identify more effective therapeutic compounds, especially phytochemicals, to improve the clinical outcome of CRC without causing any side effects.

Correspondence: Junhui Cui
Department of Coloproctological Surgery, Tongde Hospital of Zhejiang Province, 234 Gu-Cui Road, Hangzhou 310012, People's Republic of China
Tel/Fax +86 571 8997 2373
Email 13958105761@163.com

Transforming growth factor-β1 (TGF-β1), the prototypical member of the TGF-β superfamily, is a secreted pleiotropic cytokine that plays a vital role in the development and progression of CRC.[5] TGF-β1 binds to the type I and type II receptors (TGFβRI and TGFβRII), which triggers the Smads signaling pathway. TGF-β not only plays a regulatory role in the physiology of the normal colon[6] but is also a key player in CRC development, angiogenesis, progression, metastasis and immune evasion.[7,8] Not surprisingly therefore, the TGF-β/Smad regulatory axis is the target of multiple anti-CRC chemotherapeutics. Oxymatrine (OM), an alkaloid extracted from the Chinese herb Sophora flavescens Ait, inhibits in vitro migration of the human CRC RKO cell line by blocking PAI-1 and the TGF-β1/Smad signaling pathway.[9] MnTE-2-PyP is a superoxide dismutase (SOD) mimetic that inhibits TGF-β1-induced changes in CRC cells through the Smad2/3 signaling pathway,[10] while the plant-derived steroid ginsenoside Rb2 inhibits epithelial mesenchymal transition (EMT) through this pathway as well.[5] Celastrol, an anti-inflammatory phyto-terpenoid,

reduced the expression levels of TGF-β1, TGFβRI and TGFβRII, and also prevented the increase in Smad4 and p-Smad2/3 in HCT116 and SW620 cells.[11] Berberine (BBR) is a potent alkaloid extracted from the bark of Berberis species, and inhibits EMT and migration of CRC cells by modulating the expression of TβRII, Smad2 and p-Smad3.[12] A number of other natural phytochemicals have shown similar anti-cancer effects.[13,14]

Oridonin (Figure 1A), an ent-kaurene diterpenoid isolated from Rabdosia rubescens, is an important active component of several Chinese medicinal formulations. Studies show multiple pharmacological and physiological effects of oridonin, such as anti inflam¬matory, anti bacterial, neuroprotective and antitumor effects.[15] In recent years, oridonin has been tested against multiple cancer types in China on account its low toxicity.[16] For instance, oridonin exerts an anti-proliferative effect on human osteosarcoma cells by inhibiting the TGF-β1/Smad2/3 signaling pathway,[17] and also induces apoptosis in CRC cells by activating either the BMP7/p38MAPK/p53 signaling pathway, or the p38/MAPK/PTEN pathway.[18,19]
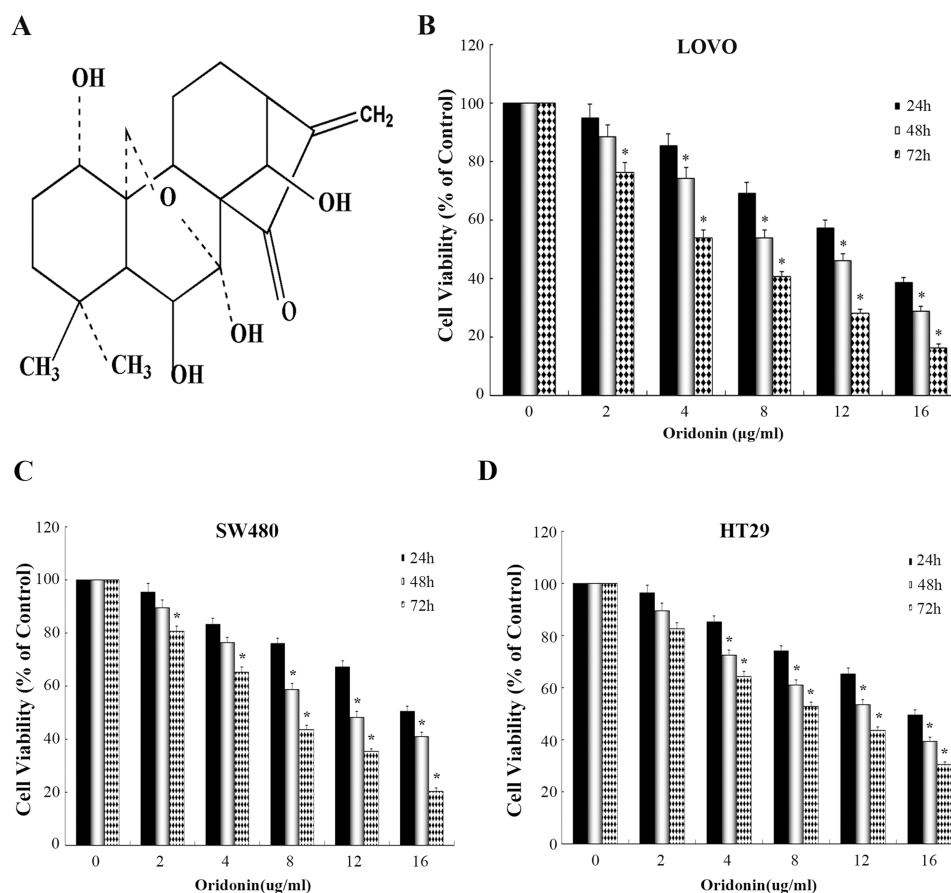
Figure 1 Effects of oridonin on the growth of colon cancer cells. (**A**) Chemical structure of oridonin. (**B-D**) The cells (including LOVO, SW480 and HT29 cells) were treated with various doses of oridonin (0–16 μg/mL) for 24, 48 or 72 h, respectively. The cell viability was determined by CCK-8 assay. *P<0.05 vs the control.

Nevertheless, the exact mechanism underlying the therapeutic action of oridonin against CRC remains to be elucidated, especially in the context of the TGF-β1/Smads signaling pathway. To this end, we analyzed the effects of oridonin in the human colon cancer LOVO cell line, and in a murine orthotopic tumor model. Our findings provide novel insights into the mechanism of oridonin, and underscores its potential in the treatment of CRC.

Materials and reagents

Oridonin (purity>98%, cat. no. A0063) was purchased from Shanghai Biotechnology Co. Ltd. and dissolved in dimethyl sulfoxide (DMSO) to prepare a 10 mM stock solution. Fetal bovine serum (FBS), 0.25% trypsin containing EDTA, DSMO, F12K medium and penicillin/streptomycin were purchased from Abcam (Cambridge, UK). TRIzol reagent, BCA protein assay kit (P0010) and RIPA lysis buffer (P0013B) were purchased from Beyotime Biotechnology (Shanghai, China). TGF-β1 was obtained from Oukai Biotechnology Co. Ltd. (Nanjing, Jiangsu). Mouse monoclonal antibodies against GAPDH (cat. no. 2118L), Smad2 (cat. no. WH098190), p-Smad2 (cat. no. 3108S) and Smad4 (cat. no. ab40759) were acquired from Cell Signaling Technology (USA), and monoclonal antibodies against PAI (cat. no. 13801-1-AP), p-Smad3 (cat. no. bs-5235R) and Smad3 (cat. no. 3463–100) from ABclonal Biotechnology Co. Ltd. (Boston, USA). Anti-mouse IgG horseradish peroxidase (HRP)-conjugated secondary antibody (cat. no. 3310-13) was purchased from Sigma (USA).

Cell culture and treatment

The colon cancer cell lines LOVO, SW480, HT29 were purchased from Enzyme Biotechnology Co. Ltd (Shanghai, China), and cultured in F12K medium supplemented with 10% FBS and antibiotics (100 units/mL penicillin, 100 μg/mL streptomycin) at 37 °C under 5% CO_2. The culture medium was replaced every 48 h, and the cells were passaged at 80% confluency. For in vitro assays, LOVO cells in the logarithmic growth period were seeded onto 6-well culture plates and allowed to adhere overnight. After replacing the complete medium with fresh serum-free F12K, and cells were starved for 6 h, and then treated with 10 ng/mL TGF-β and/or 8 ug/mL oridonin for 48 h. The cells were harvested and processed as appropriate.

Cell viability assay

Cell viability was assessed using the CCK-8 kit according to the manufacturer's instructions. Briefly, 100 μl cell suspension in the logarithmic phase was dispensed in 96-well culture plates at the density of 3×10^3 per well, and cultured overnight. The cells were treated with different concentrations (0, 2, 4, 8, 12, 16 μg/mL) of oridonin for 24, 48 or 72 h, followed by 10 μl CCK working solution per well. After incubating for 1–3 h, the absorbance at 450 nm was measured using Bio-Tek, ELX800 (USA). Each condition was tested in 6 replicates.

Experimental animals

Four to six-week old male athymic BALB/c nude mice (weighing 18–20 g) were obtained from Shanghai Slake Experimental Animals Co. Ltd., and housed in a regulated SPF environment (20–26 °C, relative humidity 40–70% and 12 h light/dark cycle) with food and water provided ad libitum. All experimental procedures and protocols were approved by the Institutional Animal Care and Use Committee of the Zhejiang Chinese Medical University. All the animal experiments were performed in accordance with the approved guidelines for welfare and ethics of Zhejiang Chinese Medical University Laboratory Animal Research Center.

Establishment of murine orthotopic CRC model

Briefly, each mouse was injected subcutaneously with 0.2 mL of 1×10^7/mL LOVO cell suspension into the right flank, and euthanized once the tumor grew to 1 cm^3. The tumors were excised, cleaned off of the peripheral connective tissue, and minced into 1 mm^3 pieces in sterile saline containing penicillin (120 units/mL). To establish the orthotopic transplantation model, 24 nude mice were anesthetized, and a longitudinal incision was made in their right lower abdomen. The colon was carefully removed, the serosa was peeled off, and the primary tumor pieces were inserted and sutured transversely with a 7-0 silk thread. The colon was put back into the abdominal cavity, and the incision was sutured with 4-0 silk thread. One week after orthotopic transplantation, the mice were randomly divided into the control and oridonin-treated groups (5 mice/group), and intraperitoneally injected with 50 μl of 0.9% sodium chloride or different doses (2.5 mg/kg, 5 mg/kg and 7.5 mg/kg) of oridonin once a day for two weeks. The day after the last injection, the mice were euthanized, and the tumors were removed and weighed with electronic scale. The diameters of the tumor samples were measured with digital calipers, the volume of a tumor was calculated using the following formula: Tumor volume (cm^3) = longer diameter x shorter diameter^2/2. Each tumor

was cut into two pieces, and one half was fixed with 10% formalin and the other half was flash frozen in liquid nitrogen.

Reverse transcription PCR (RT-PCR)

The total RNA was extracted from the cultured cells and frozen tumor tissues by TRIzol reagent, and the purity and concentration of RNA were determined by UV spectrophotometry (Spectro Art 200, Wealtec corporation, USA). The cDNA was synthesized using RevertAid First Strand cDNA synthesis Kit (Thermo Fisher Scientific, USA, cat. no. K1622). PCR was performed by Real-Time PCR Detection System (BIO-RAD, USA) using the following conditions: 95 °C for 3 min (pre-denaturation), 40 cycles at 95 °C for 10 s, 60 °C for 20 s and 72 °C for 30 s, and final extension at 72 °C for 10 min. GAPDH was used as the internal control. The specific primers were designed using the Gene Runner software and synthesized by Beijing Aoke Biotechnology Co. Ltd. (Beijing, China) (Table 1). The PCR products were detected by 1% agarose gel electrophoresis, and the gel images were analyzed by Image J software.

Western blotting analysis

The harvested cells or frozen tumor tissues were lysed in RIPA buffer. The total protein concentration was determined using the BCA Protein Assay Kit. Equivalent amount of protein (40 μg/lane) from each sample was separated by 12% polyacrylamide gel electrophoresis, and transferred to PVDF membrane (Millipore, USA). After blocking with 5% skim milk in TBST (10 mM

Tris, 150 mM NaCl, 0.05% Tween-20) at 37 °C for 2 hrs, the blots were washed and incubated overnight with primary antibodies against GAPDH (1:5000), Smad2 (1:500–1:2000), p-Smad2 (1:1000), Smad4 (1:1000), PAI (1:500–1:1000), Smad3(1:1000) and p-Smad3 (1:1000) at 4 °C. The membranes were washed thrice with 1X TBST and then incubated with horseradish peroxidase-conjugated secondary antibodies (1:10000) for 2 h at room temperature. After washing thrice with 1X TBST, the bands were visualized using ECL Plus chemiluminescence reagent Kit (Bio-Rad, USA), and their optical density was measured by Image J software.

Hematoxylin-eosin (HE) staining and immunohistochemistry (IHC)

The formalin-fixed tissues were embedded in paraffin, and cut into 5 μm-thick sections. The latter were deparaffinized in xylene and hydrated through an alcohol gradient. HE staining was performed as per standard protocols, and the sections were viewed under a light microscope (DMIL LED Fluo S/N 418544, LEICA Inc.). For IHC, the sections were processed as above, boiled in EDTA (PH 8) for 20 mins for antigen retrieval, and then incubated with 3% H_2O_2 for 10 mins to block endogenous peroxidase activity. The sections were then incubated overnight with the primary antibodies against PAI-1 (1:100), Smad3 (1:100), Smad2 (1:100) and Smad4 (1:100) at 4 °C, washed thrice with PBS and then incubated with the corresponding secondary antibody for 20 min at 37 °C. PBS as used in place of the primary antibody as negative control. The sections were developed using DAB, and then counterstained

Table 1 Primer sequences used for RT-PCR analysis

Genes		Primer sequences	Product size (bp)
TGF-β1	Forward Reverse	5'-CAATTCCTGGCGATACCTCAG-3' 5'-GCACAACTCCGGTGACATCAA-3'	308
Smad2	Forward Reverse	5'-TGCCGATTATGGCGCTGGC-3' 5'-GAGTGAGGGCTGTGATGCATG-3'	507
Smad3	Forward Reverse	5'-AACAACCAGGAGTTCGCTGC-3' 5'-GGACCTTGTCAAGCCACTGC-3'	102
Smad4	Forward Reverse	5'-ACATACAGCACCCCAGCTCTG-3' 5'-GTCTCTCCTACCTGAACATCCAT-3'	434
PAI-1	Forward Reverse	5'- AAAGGAGCCGTGGACCAGC-3' 5'- TTGGTGAGGGCAGAGAGAGGC-3'	296
GAPDH	Forward Reverse	5'- GCAGGGGGGAGCCAAAAGG-3' 5'- GGCCCTCCGACGCCTG-3'	470

with hematoxylin. The stained slides were dehydrated and mounted with neutral balsam (Absin Bioscience Inc. shanghai), and observed under the microscope. The results were analyzed by Image Pro Plus software.

Statistical analysis

All data were expressed as mean ± standard deviation (SD) of at least three independent tests. Statistical comparison was made by one-way analysis of variance (multiple groups) or Student's t-test (two groups) using the SPSS 18.0 software. P-values less than 0.05 were considered statistically significant.

Results
Effects of oridonin on cell viability of colon cancer cells

As illustrated in Figure 1B–D. Results demonstrated that antiproliferation activitiy of oridonin on LOVO cell line was dose- and time-dependent manner and significantly higher than other cell lines. Half-maximal cytotoxicity of oridonin on LOVO

cells was ~8–12 μg/mL at 48 h. On the basis of these results, The LOVO cells were selected for subsequent experiments.

Effects of oridonin on TGF-β1-induced Smad signaling, PAI-1 in LOVO cells

To elucidate whether oridonin affected the TGF-β1/Smad pathway in LOVO cells and explore its possible molecular mechanisms, RT-PCR and Western blotting analysis were used to detect the mRNA and protein expression levels of Smad signaling. As shown in Figure 2A and B, As compared with the control group, The mRNA expression levels of Smad2, Smad3, Smad4 and PAI-1 were significantly induced by TGF-β1, But oridonin alleviated the augment of Smad2, Smad3, Smad4 and PAI-1 expression levels in TGF-β1-treated cells. In addition, TGF-β1 similarly stimulated the protein expression levels of Smad2, p-Smad2, Smad3, p-Smad3, Smad4 and PAI-1, while oridonin restrained the increase of Smad2, Smad3, Smad4, PAI-1 expression and the phosphorylation of Smad2, Smad3 in
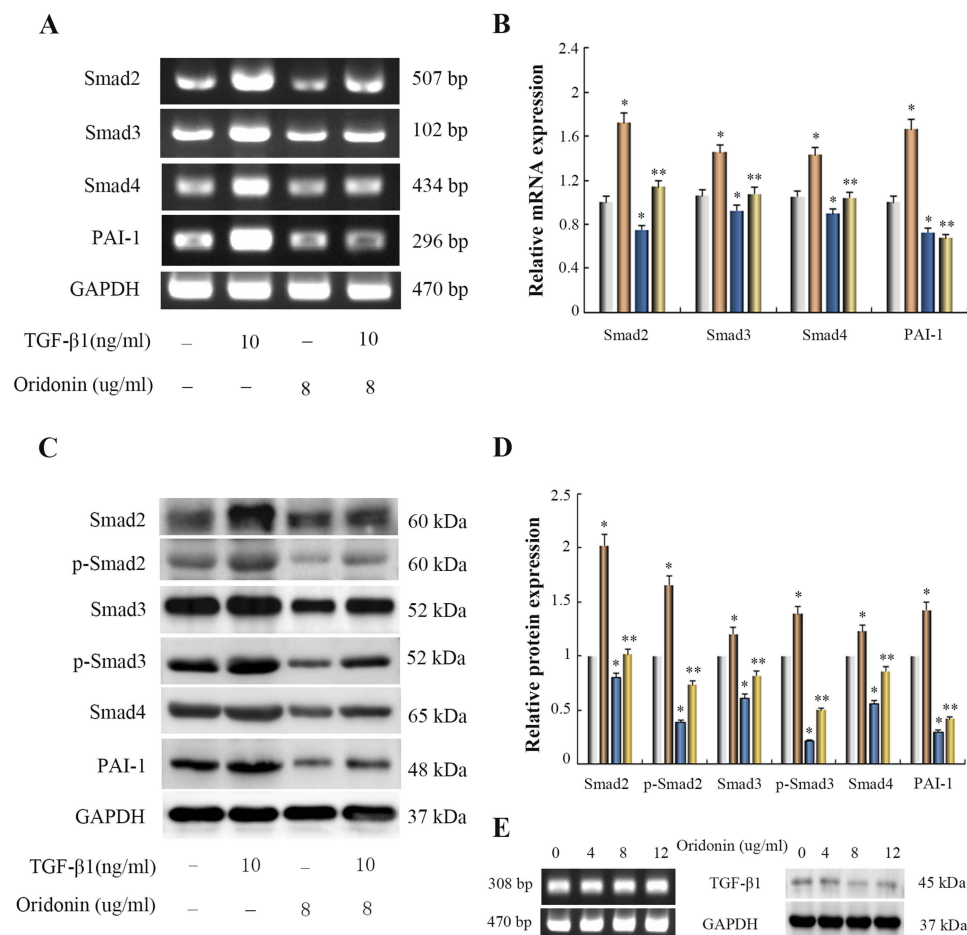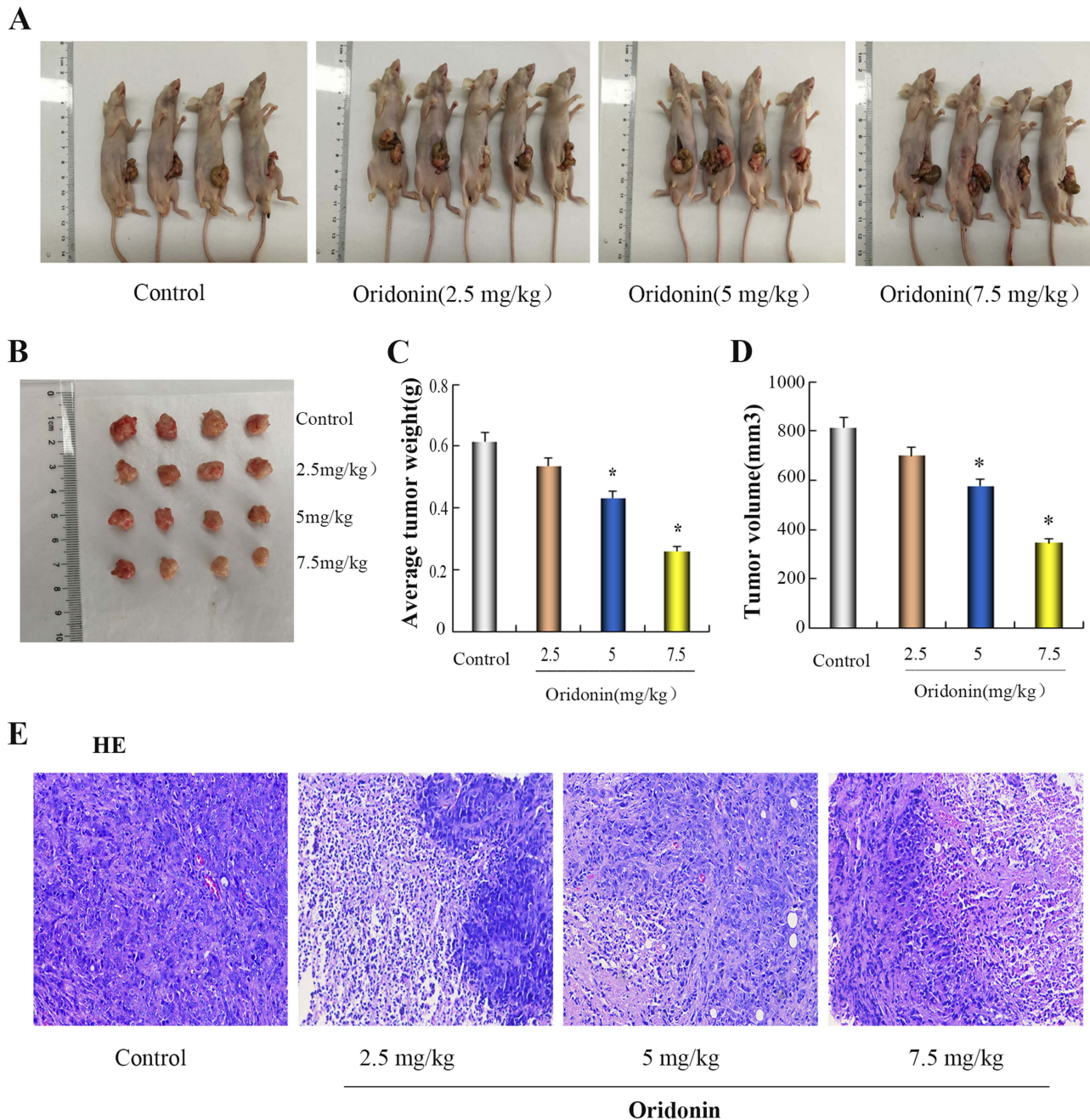

Figure 2 Effects of oridonin on the expression of Smad2, Smad3, Smad4, p-Smad2, p-Smad3 and PAI-1 in TGF-β1-indued colon cancer LOVO cells and TGF-β1 in LOVO cells. Cells were exposed to oridonin (8 μg/mL) or/and 10 ng/mL TGF-β for 48 h. (**A, C** and **E**) Results of RT-PCR and Western blotting analysis. (**B** and **D**) The relative quantification of Densitometric analyses. *P<0.05 vs control group; *P<0.05 vs TGF-β1-treated group.

TGF-β1-treated cells (Figure 2C and D). Interestingly, we found that oridonin had no significant effect on mRNA expression of TGF-β1 in LOVO cells with increasing concentration (Figure 2E). In addition, the protein of TGF-β1 in LOVO cells was almost not expressed, and oridonin at different concentrations had no effect on protein expression of TGF-β1 (Figure 2E). These results suggested that oridonin inhibited the LOVO cell growth,

at least in part, via inactivation of Smad signaling pathway.

Oridonin inhibited the growth of orthotopically transplanted colon cancer

To further explore the effect of oridonin on tumor growth in vivo, Orthotopic nude mouse models of LOVO cells were performed. As was shown in Figure 3A–D, After

A

Control   Oridonin(2.5 mg/kg)   Oridonin(5 mg/kg)   Oridonin(7.5 mg/kg)

B

C

D

E   **HE**

Control   2.5 mg/kg   5 mg/kg   7.5 mg/kg

Oridonin

Figure 3 Antitumor effect of oridonin in vivo. (**A** and **B**) On the following day after the last treatment, orthotopically implanted tumors were excised from the animals. (**C** and **D**) The bar chart showed the tumor mean weight and volume in individual groups. (**E**) morphological changes of tumor tissues were photographed in fluorescence microscope (× 200). *$P<0.05$ vs the control.

treatment with oridonin(2.5 mg/kg, 5 mg/kg, 7.5 mg/kg), mean tumor weight and volume in oridonin-treated groups were reduced compared with those in the control groups. the inhibition ratio reached 12.7%, 29.6% and 57.5%, respectively. However, that in oridonin(5 mg/kg and 7.5 mg/kg)-treated group was significantly lower than those of the control and oridonin(2.5 mg/kg)-treated group($P<0.05$). No significant difference were observed in the oridonin(2.5 mg/kg)-treated group and the control group ($P>0.05$). Therefore, tumor growth was effectively suppressed in tumor-bearing mice after treatment with 5 mg/kg oridonin.

In order to further investigate the anti-tumor effect in vivo, HE staining was applied to observe the morphological changes of tumor tissues. The results in Figure 3E showed that the morphology and size of the cells were different, the arrangement of the cells was disordered, the nucleus of the tumor cells were large, the cytoplasms were deep stained, and vascular tissue was seen in the stromain the control group. There were no significant changes in tumor morphology in the oridonin-treated groups compared with the saline-treated group, but irregular necrotic areas appeared in the parenchyma of the tumor tissue.

Effects of oridonin on the protein expression of Smad2, Smad3, Smad4, PAI-1 in tumor tissues

To confirm wether oridonin exerted anti-tumor effects through regulating Smad pathway in vivo, Immunohistochemical analysis was used to investigate the protein expression levels of Smad2, Smad3, Smad4 and PAI-1. The results(Figure 4) revealed that different doses of oridonin decreased the expression levels of Smad2, Smad3, Smad4 and PAI-1 compared with control group in tumor tissues ($P<0.05$). Similarly, As was shown in Figure 6A and B, Western blotting analysis was further used to confirm that oridonin treatment suppressed the expression levels of Smad2, Smad3, Smad4, p-Smad2, p-Smad3, PAI-1 compared with control group in tumor tissues, with significant difference between 5 mg/kg, 7.5 mg/kg and control group ($P<0.01$).

Effects of oridonin on the mRNA expression of Smad2, Smad3, Smad4, PAI-1 in tumor tissues

Consistent with the differential expression in protein levels, the results of RT-PCR detection also indicated that treatment with oridonin caused a decrease of Smad2, Smad3, Smad4, PAI-1 in mRNA levels in a dose-dependent manner (Figure 5A and B), and the expression levels were significantly lower in 5 mg/kg and 7.5 mg/kg than that in control group ($P<0.01$).

Discussion

Colorectal cancer (CRC) is a highly prevalent and fatal malignancy, which is frequently associated with poor prognosis, mostly due to post-therapeutic metastasis.[4] Despite the numerous studies conducted in recent years, the regulatory mechanism are still unclear. In present study, we found that oridonin effectively suppressed the proliferation of LOVO cells in vitro, and inhibited the growth of orthotopically implanted tumors. Mechanistically, oridonin lowered the levels of Smad2, Smad3, Smad4 and PAI-1, and decreased the phosphorylation of Smad2 and Smad3 in a dose-dependent manner. Thus, we have shown for the first time that oridonin inhibits CRC cell growth by blocking the TGF-β1/Smads- PAI-1 signaling pathway.

The TGFβ family consists of the TGF-β cytokines, bone morphogenetic protein (BMP) and growth differentiate factor (GDF) among others.[20] In the early stages of tumorigenesis, the TGF-β pathway inhibits tumor formation. However, as the tumor cells undergo EMT and acquire the ability of invade and metastasize,[21] the surface expression levels of TβRI and TβRII are aberrantly increased.[22] TGF-β1 recognizes and binds to the constitutively active TβRII, which then binds to and phosphorylates TβRI.[23,24] The latter then phosphorylates downstream effectors such as the Smad proteins, which play a crucial role in the canonical TGF-β signal pathway.[25] TGF-β receptors directly activate Smad2 and/or Smad3, which then form a complex with Smad4 that translocates into the nucleus, and regulates the expression of several genes.[17] We found that oridonin inhibited the levels of total and phosphorylated Smad proteins in the TGF-β1-treated LOVO cells, indicating that its anti-proliferative effects were mediated via deactivation of the TGF-β1/Smad signaling pathway.

PAI-1, a single-chain glycoprotein of the SERPIN superfamily, is the primary and most specific inhibitor of both the tissue-type plasminogen activator (t-PA) and the urinary-type plasminogen activator (u-PA),[26] and is regulated by cytokines, growth factors, cellular stress etc. Recent studies implicate a more pleiotropic role of PA-1 involving tumorigenesis, cell migration, invasion, adhesion and angiogenesis,[27] and there are reports of its direct
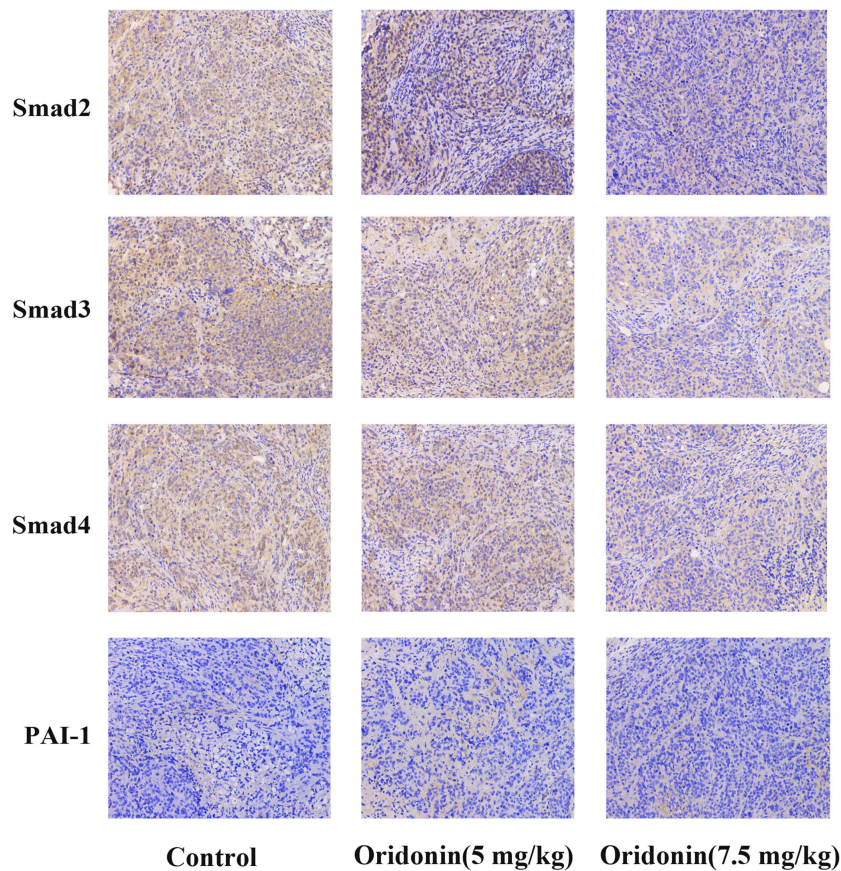
Figure 4 Expressions of Smad2, Smad3, Smad4 and PAI-1 were analyzed by immunohistochemistry. Results of the mean optical densities measured in the orthotopic transplanted tumor tissues from the mice following treatment without (control) or with different doses of oridonin. Magnification: 200×.
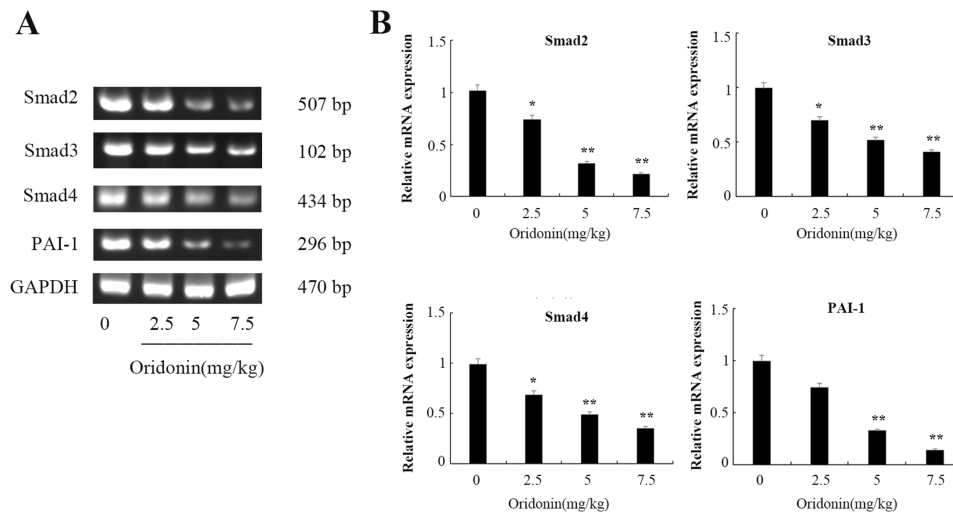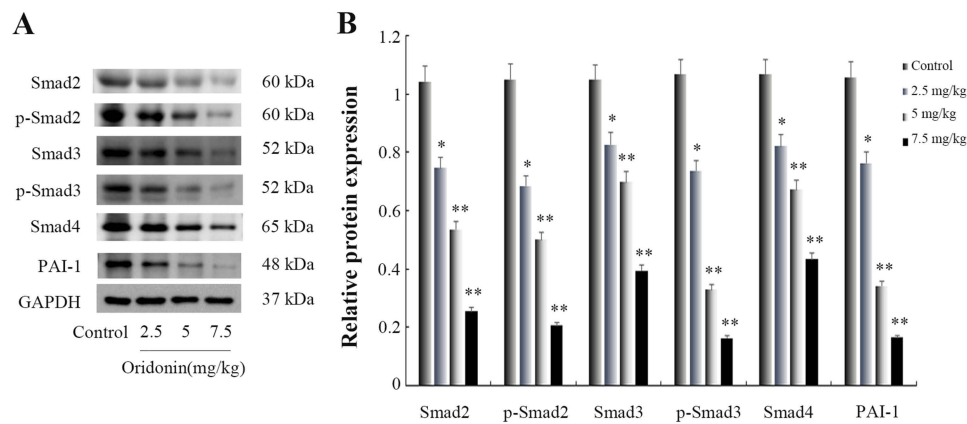

Figure 5 Effects of oridonin on the mRNA expression of Smad2, Smad3, Smad4 and PAI-1 in xenograft tumor tissues. (**A**) Results of RT-PCR analysis in tumor tissues. (**B**) Quantified data of densitometric analyses. *P<0.05, **P<0.01 as compared with the control group.

as well as indirect influence on tumor progression.[28–30] PAI-1 is an effective regulator of tumor growth in vivo[31] and is elevated in many solid tumor types including CRC, and associated with poor prognosis.[32–34] Therefore, it is a promising therapeutic target for a variety of cancers. PAI-1 is effectively induced by the TGF-β1/Smad pathway[35,36]

Figure 6 Effects of oridonin on the protein expression of Smad2, Smad3, Smad4, p-Smad2, p-Smad3 and PAI-1 in xenograft tumor tissues. (**A**) Results of Western blotting analysis in tumor tissues. (**B**) Quantified data of densitometric analyses. *$P<0.05$, **$P<0.01$ as compared with the control group.

through a Smad binding element (SBE) on the PA-1 promoter, and triggers the degradation of the extracellular matrix, which in turn facilitates cell invasion and migration.[37] Consistent with previous reports, PAI-1 levels were markedly increased in TGF-β1-treated LOVO cells, and inhibited upon oridonin pre-treatment, which suggests that the latter inhibits TGF-β1-mediated upregulation of PAI-1 by inhibiting the nuclear translocation of Smad2 and Smad3. The in vitro results were validated by the significant reduction in the orthotopic tumor growth in the oridonin-treated mice, along with marked alterations in the in situ levels of Smads and PAI-1. Taken together, oridonin restrains CRC growth by hindering the TGF-β1/Smads-PAI-1 signaling pathway, and is a promising chemotherapeutic agent against colon tumors.

Conclusion

Oridonin exhibited inhibitory effects on colon cancer in vitro and in vivo. The mechanism might be due to the deactivation of the TGF-β1/Smads-PAI-1 signaling pathway. These findings suggest that oridonin can be used as a potential natural drug in treatment for patients with CRC.

Acknowledgment

Disclosure

The authors report no conflicts of interest in this work.

References

1. Wong KE, Ngai SC, Chan K-G, Lee L-H, Goh B-H, Chuah L-H. Curcumin nanoformulations for colorectal cancer: a review. *Front Pharmacol*. 2019;10:152. doi:10.3389/fphar.2019.00848
2. Pan R, Zhu M, Yu C, et al. China Kadoorie Biobank Collaborative Group. Cancer incidence and mortality: a cohort study in China, 2008–2013. *Int J Cancer*. 2017;141(7):1315–1323. doi:10.1002/ijc.30825
3. Choi Y, Sateia HF, Peairs KS, Stewart RW. Screening for colorectal cancer. *Semin Oncol*. 2017;44(1):34–44. doi:10.1053/j.seminoncol.2017.02.002
4. Sheng N, Yan L, Kai W, et al. TRIP13 promotes tumor growth and is associated with poor prognosis in colorectal cancer. *Cell Death Dis*. 2018;9(3):402. doi:10.1038/s41419-018-1111-y
5. Dai G, Sun B, Gong T, Pan Z, Meng Q, Ju W. Ginsenoside Rb2 inhibits epithelial-mesenchymal transition of colorectal cancer cells by suppressing TGF-β/Smad signaling. *Phytomedicine*. 2018;56:126–135. doi:10.1016/j.phymed.2018.10.025
6. Villalba M, Evans SR, Vidal-Vanaclocha F, Calvo A. Role of TGF-β in metastatic colon cancer: it is finally time for targeted therapy. *Cell Tissue Res*. 2017;370(1):29–39. doi:10.1007/s00441-017-2633-9
7. Chruścik A, Gopalan V, Lam AK. The clinical and biological roles of transforming growth factor beta in colon cancer stem cells: a systematic review. *Eur J Cell Biol*. 2018;97(1):15–22. doi:10.1016/j.ejcb.2017.11.001
8. Tauriello DVF, Palomo-Ponce S, Stork D, et al. TGFβ drives immune evasion in genetically reconstituted colon cancer metastasis. *Nature*. 2018;554(7693):538–543. doi:10.1038/nature25492
9. Wang X, Liu C, Wang J, Fan Y, Wang Z, Wang Y. Oxymatrine inhibits the migration of human colorectal carcinoma RKO cells via inhibition of PAI-1 and the TGF-β1/Smad signaling pathway. *Oncol Rep*. 2017;37(2):747–753. doi:10.3892/or.2016.5292
10. Yang Y, Zhang P, Yan R, et al. MnTE-2-PyP attenuates TGF-β-induced epithelial-mesenchymal transition of colorectal cancer cells by inhibiting the Smad2/3 signaling pathway. *Oxid Med Cell Longev*. 2019;2019:8639791. doi:10.1155/2019/8639791
11. Jiang Z, Cao Q, Dai G, et al. Celastrol inhibits colorectal cancer through TGF-β1/Smad signaling. *Onco Targets Ther*. 2019;12:509–518. doi:10.2147/OTT.S187817
12. Huang C, Tao L, Wang XL, Pang Z. Berberine reversed the epithelial-mesenchymal transition of normal colonic epithelial cells induced by SW480 cells through regulating the important components in the TGF-β pathway. *J Cell Physiol*. 2019;234(7):11679–11691. doi:10.1002/jcp.27835

13. Maggioni D, Biffi L, Nicolini G, Garavello W. Flavonoids in oral cancer prevention and therapy. *Eur J Cancer Prev*. 2015;24:517–528. doi:10.1097/CEJ.0000000000000109

14. Merarchi M, Sethi G, Shanmugam MK, Fan L, Arfuso F, Ahn KS. Role of natural products in modulating histone deacetylases in cancer. *Molecules*. 2019;24(6):pii: E1047. doi:10.3390/molecules24061047

15. Xu J, Wold EA, Ding Y, Shen Q, Zhou J. Therapeutic potential of oridonin and its analogs: from anticancer and antiinflammation to neuroprotection. *Molecules*. 2018;23(2):pii: E474. doi:10.3390/molecules23020474

16. Li D, Han T, Liao J, et al. Oridonin, a promising ent-Kaurane diterpenoid lead compound. *Int J Mol Sci*. 2016;17:17.

17. Sun Y, Jiang X, Lu Y, et al. Oridonin prevents epithelial-mesenchymal transition and TGF-β1-induced epithelial-mesenchymal transition by inhibiting TGF-β1/Smad2/3 in osteosarcoma. *Chem Biol Interact*. 2018;296:57–64. doi:10.1016/j.cbi.2018.09.013

18. Liu RX, Ma Y, Hu XL, et al. Anticancer effects of oridonin on colon cancer are mediated via BMP7/p38 MAPK/p53 signaling. *Int J Oncol*. 2018;53(5):2091–2101. doi:10.3892/ijo.2018.4527

19. Wu QX, Yuan SX, Ren CM, et al. Oridonin upregulates PTEN through activating p38 MAPK and inhibits proliferation in human colon cancer cells. *Oncol Rep*. 2016;35(6):3341–3348. doi:10.3892/or.2016.4735

20. Zhang L, Wang X, Lai C, Zhang H, Lai M. PMEPA1 induces EMT via a non-canonical TGF-β signalling in colorectal cancer. *J Cell Mol Med*. 2019;23(5):3603–3615. doi:10.1111/jcmm.14261

21. Pickup M, Novitskiy S, Moses HL. The roles of TGFβ in the tumour microenvironment. *Nat Rev Cancer*. 2013;13(11):788-799. doi:10.1038/nrc3603

22. Luo J, Chen XQ, Li P. The role of TGF-β and its receptors in gastrointestinal cancers. *Transl Oncol*. 2019;12(3):475–484. doi:10.1016/j.tranon.2018.11.010

23. Yan X, Liao H, Cheng M, et al. Smad7 protein interacts with receptor-regulated Smads (R-Smads) to inhibit transforming growth factor-β (TGF-β)/Smad signaling. *J Biol Chem*. 2016;291:382–392. doi:10.1074/jbc.M115.694281

24. Ma M, He M, Jiang Q, et al. MiR-487a promotes TGF-β1-induced EMT, the migration and invasion of breast cancer cells by directly targeting MAGI2. *Int J Biol Sci*. 2016;12:397–408. doi:10.7150/ijbs.13475

25. Da C, Liu Y, Zhan Y, Liu K, Wang R. Nobiletin inhibits epithelial-mesenchymal transition of human non-small cell lung cancer cells by antagonizing the TGF-β1/Smad3 signaling pathway. *Oncol Rep*. 2016;35:2767–2774. doi:10.3892/or.2016.4661

26. Cesari M, Pahor M, Incalzi RA. Plasminogen activator inhibitor-1 (PAI-1): a key factor linking fibrinolysis and age-related subclinical and clinical conditions. *Cardiovasc Ther*. 2010;28:e72–91. doi:10.1111/j.1755-5922.2010.00171.x

27. Giacoia EG, Miyake M, Lawton A, Goodison S, Rosser CJ. PAI-1 leads to G1-phase cell-cycle progression through cyclin D3/cdk4/6 upregulation. *Mol Cancer Res*. 2014;12(3):322–334. doi:10.1158/1541-7786.MCR-13-0543

28. Placencio VR, DeClerck YA. Plasminogen activator inhibitor-1 in cancer: rationale and insight for future therapeutic testing. *Cancer Res*. 2015;75(15):2969–2974. doi:10.1158/0008-5472.CAN-15-0876

29. Gramling MW, Church FC. Plasminogen activator inhibitor-1 is an aggregate response factor with pleiotropic effects on cell signaling in vascular disease and the tumor microenvironment. *Thromb Res*. 2010;125(5):377–381. doi:10.1016/j.thromres.2009.11.034

30. Czekay RP, Wilkins-Port CE, Higgins SP, et al. PAI-1: an integrator of cell signaling and migration. *Int J Cell Biol*. 2011;2011:562481. doi:10.1155/2011/562481

31. Iwaki T, Urano T, Umemura K. PAI-1, progress in understanding the clinical problem and its aetiology. *Br J Haematol*. 2012;157(3):291–298. doi:10.1111/j.1365-2141.2012.09074.x

32. Tong Q, Weaver MR, Kosmacek EA, et al. MnTE-2-PyP reduces prostate cancer growth and metastasis by suppressing p300 activity and p300/HIF-1/CREB binding to the promoter region of the PAI-1 gene. *Free Radic Biol Med*. 2016;94:185–194. doi:10.1016/j.freeradbiomed.2016.02.036

33. Lampelj M, Arko D, Cas-Sikosek N, et al. urokinase plasminogen activator (uPA) and plasminogen activator inhibitor type-1 (PAI-1) in breast cancer–correlation with traditional prognostic factors. *Radiol Oncol*. 2015;49:357–364. doi:10.2478/raon-2014-0049

34. Deepak V, Ramachandran S, Balahmar RM, et al. In vitro evaluation of anticancer properties of exopolysaccharides from Lactobacillus acidophilus in colon cancer cell lines. *In Vitro Cell Dev Biol Anim*. 2016;52:163–173. doi:10.1007/s11626-015-9970-3

35. Chen C, Sun MZ, Liu S, et al. Smad4 mediates malignant behaviors of human ovarian carcinoma cell through the effect on expressions of E-cadherin, plasminogen activator inhibitor-1 and VEGF. *BMB Rep*. 2010;43:554–560. doi:10.5483/bmbrep.2010.43.8.554

36. Zhu Y, Yin WL, Ba YF, et al. Transforming growth factor-1 promotes the transcriptional activation of plasminogen activator inhibitor type1 in carcinoma-associated fibroblasts. *Mol Med Rep*. 2012;6:1001–1005. doi:10.3892/mmr.2012.1020

37. Goto N, Hiyoshi H, Ito I, et al. Identification of a novel compound that suppresses breast cancer invasiveness by inhibiting transforming growth factor-β signaling via estrogen receptor α. *J Cancer*. 2014;5:336–343. doi:10.7150/jca.7202